Med Chem Res
DOI 10.1007/s00044-017-1806-0

MEDICINAL CHEMISTRY RESEARCH

ORIGINAL RESEARCH

Synthesis of 2-phenyl-1*H*-imidazo[4,5-*b*]pyridine as type 2 diabetes inhibitors and molecular docking studies

Muhammad Taha[1,2] · Nor Hadiani Ismail[1,2] · Syahrul Imran[1,2] · Izzatul Ainaa[2] · Manikandan Selvaraj[3,4] · Mohd syukri baharudin[1,2] · Muhammad Ali[5] · Khalid Mohammed Khan[6] · Nizam Uddin[7]

Received: 29 August 2016 / Accepted: 13 February 2017

Abstract A series of imidazo[4,5-*b*]pyridines (**3–32**) was synthesized and evaluated for their ability to inhibit Baker's yeast α-glucosidase enzyme. The IC_{50} values for all compounds were in the range of 13.5–93.7 µM with compound **15**, a 2,4-dihydroxy-substituted analog, displayed the most potent activity potential. Structure–activity relationship strongly suggested the presence of hydroxyl group at aromatic side chain as the main contributing factor towards the inhibitory potential. Findings also suggested that compounds having hydroxyl groups at *ortho* and *para* positions are able to inhibit α-glucosidase enzyme efficiently. This experimental observation was further supported by docking studies carried out on human intestinal maltase-glucoamylase enzyme (PDB ID: 3TOP). The –NH– group of imidazo-pyridine of compound **15** formed H-bond with Asp1526, while both hydroxyls of catechol formed H-bond with Asp1279. Imidazo-pyridine ring was well stabilized by π–π stacking with Phe1560, and other hydrophobic interactions involving side chain of Pro1159, Tyr1167, Asp1157, Met1421, Trp1369, Pro1318, and Lys1460. The catechol ring also forms several hydrophobic interactions with Phe1560, Trp1523, Trp1418, His1584, Try1251, Ile1218 and Trp1355.

Keywords Imidazo[4,5-*b*]pyridine · Type-2 Diabetes · Pharmacokinetic prediction · Molecular docking

Electronic supplementary material The online version of this article (doi:10.1007/s00044-017-1806-0) contains supplementary material, which is available to authorized users.

✉ Muhammad Taha
taha_hej@yahoo.com
muhamm9000@puncakalam.uitm.edu.my

1 Atta-ur-Rahman Institute for Natural Product Discovery, Universiti Teknologi MARA (UiTM), Puncak Alam Campus, Bandar Puncak Alam 42300 Selangor, Malaysia

2 Faculty of Applied Science Universiti Teknologi MARA (UiTM), 40450 Shah Alam, Selangor, Malaysia

3 Integrative Pharmacogenomics Institute (iPROMISE), Universiti Teknologi MARA (UiTM), Puncak Alam Campus, Bandar Puncak Alam 42300 Selangor Darul Ehsan, Malaysia

4 Faculty of Pharmacy, Universiti Teknologi MARA (UiTM), Puncak Alam Campus, Bandar Puncak Alam 42300 Selangor Darul Ehsan, Malaysia

5 Department of Chemistry, COMSATS Institute of Information Technology, University Road, Abbottabad, Khyber Pakhtunkhwa 22060, Pakistan

6 H. E. J. Research Institute of Chemistry, International Center for Chemical and Biological Sciences, University of Karachi, Karachi 75270, Pakistan

7 Batterje Medical College for Science & Technology, Jeddah 21442, Kingdom of Saudi Arabia

Introduction

Diabetes mellitus is a metabolic disorder that increases blood glucose levels (hyperglycemia), resulting in various medical complications like retinopathy, cardiovascular problems, nephropathy and neuropathy (Chen et al. 2013). The number of diabetes mellitus patients increased from 153 million to 347 million between the years 1980–2008 (Danaei et al. 2011), while the International Diabetes Federation estimated an increase up to 552 million by the year 2030 (Whiting et al. 2011). Type-II diabetes mellitus, common in developed countries, is resulted from reduced and impaired insulin secretion (Porte 1991; Taylor et al.

Published online: 22 February 2017

1994; Butler et al. 2003; Wu 2007; Tang et al. 2010). This is usually controlled by suppressing absorption and digestion of dietary carbohydrates, through inhibition of digestive enzymes like α-glucosidase and α-amylase (Wang et al. 2010). Glucose produced through hydrolysis of carbohydrates by α-glucosidase is being absorbed into blood stream, thus increases postprandial blood glucose level. Considered as a crucial target for drug, the inhibition of α-glucosidase can be an effective strategy in controlling type-II diabetes mellitus (Puls et al. 1977; Shim et al. 2003; Samad et al. 1988; O'Dea and Turton 1985). Current regiment for α-glucosidase inhibitors blocks glucose production by occupying the active site and prevents hydrolysis of α-(1–4)-linked *D*-glucose residues from the non-reducing end (Charron et al. 1986). This reduces the rate of glucose absorption and, therefore, decreases plasma glucose level. α-Glucosidase inhibition has attracted plenty of attention from pharmaceutical industry as a treatment method of diseases like diabetics, viral infections, hepatitis and cancer (Humphries et al. 1986; Park et al. 2008; Storr et al. 2008). Although many α-glucosidase inhibitors have been reported, most of them are sugars or sugar-derived such as acarbose (Lefebvre and Scheen 1994). In recent times, number of α-glucosidase inhibitors were discovered and studied, with several non-saccharide compounds including substrate analogs (Luo et al. 2001; Kumar et al. 2011; Wehmeier and Piepersberg 2004), which are taken orally for the treatment of diabetes. Currently available α-glucosidase inhibitors like miglitol (Scott and Spencer 2000), voglibose (Matsuo et al. 1992), acarbose (Schmidt et al. 1977) and nojirimycin (Asano et al. 1994) are having some unwanted side effects such as diarrhea, abdominal distension, meteorism, hepatoxicity and flatulence (Hsiao et al. 2006; Hollander 1992). Due to these limitations and associated absorptivity issues, (Reuser and Wisselaar 1994; Scheen 2003), new and potent α-glucosidase inhibitors are highly desired. To overcome the undesired, plenty of efforts have been put in to design and develop more effective non-glycosidic-based α-glucosidase inhibitors (Adisakwattana et al. 2004).

In the present study, a library of compounds (**3–32**) consisting of imidazopyridine scaffold has been synthesized. Imidazo[4,5-*b*]pyridine, which contains a fused imidazole ring, is reported for various activities such as antibacterial (Mallemula et al. 2013), anticancer (Temple et al. 1987), antitubercular (Bukowski and Kaliszan 1991), antiulcer (Loriga et al. 1992), analgesic (Clark et al. 1978) and antioxidant (Lavanya et al. 2011). Compounds having heterocyclic rings possess versatile biological properties and easily interact with the nature (Narasimhan et al. 2011; Imran et al. 2015a; Taha et al. 2015a; Taha et al. 2016a, 2016b). Imidazole has also been reported to show in vivo antihyperglycemic activity for treatment of type-II diabetes mellitus by stimulating insulin secretion and decreasing insulin resistance of peripheral tissues via reduction of hyperglycemia (Plant and Henquin 1990). Interestingly, it has been found that imidazole moiety is additionally considered significant for antidiabetic activity (Brownson and Hipkiss 2000). Encouraged by these previous findings, we decided to identify new α-glucosidase inhibitors and reveal new perspectives in the biological potentials of newly synthesized imidazo[4,5-*b*]pyridine. α-Glucosidase inhibitory potential of imidazo[4,5-*b*]pyridines and related compounds with similar pharmacophores like benzothiazole (A) (Taha et al. 2015b) Quinoline (B) (Taha et al. 2015c), benzimidazole (C) (Taha et al. 2016), benzimidazole thiourea (D) (Zawawi et al. 2017) have been widely reported (Fig. 1).

Material and Methods

NMR experiments were performed on Ultra Shield Bruker FT NMR 500 MHz, CHN analysis was performed on a

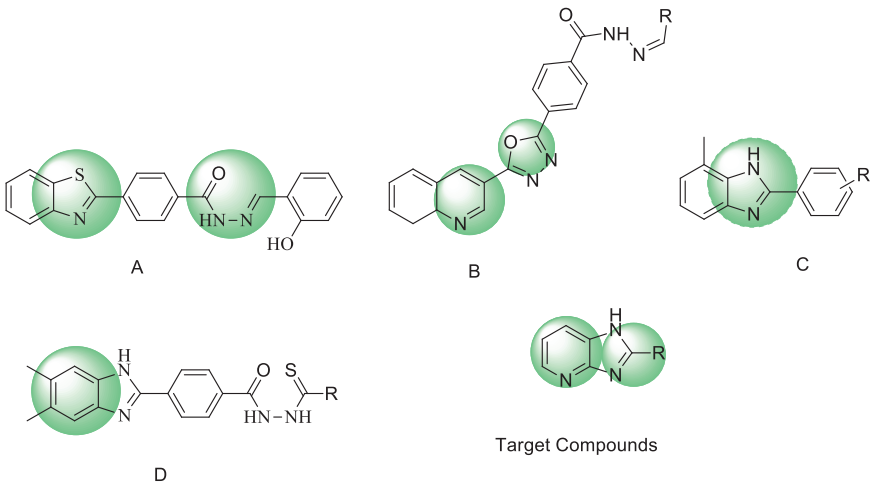

Fig. 1 Structures **a–e** similar with target compounds recently published

Carlo Erba Strumentazion-Mod-1106, Italy. Electron impact mass spectra (EI-MS) were recorded on a Finnigan MAT-311A, Germany. Thin layer chromatography was performed on pre-coated silica gel aluminum plates (Kieselgel 60, 254, E. Merck, Germany). Chromatograms were visualized using UV at 254 and 365 nm.

Synthesis

*2-Phenyl-1*H-*imidazo[4,5-b]pyridines (**3–31**)*

Equimolar amount of 5-bromopyridine-2,3-diamine **1**, benzaldehydes **2** and sodium metabisulfite were dissolved in 40 ml of Dimethylformamide and refluxed at 130 °C for 6 h. Then reaction mixture was poured into ice water to allow product precipitation. The precipitate was filtered and crystallized from ethanol to afford pure product.

*4-(6-Bromo-1*H-*imidazo[4,5-b]pyridin-2yl) phenol (**1**)*

Yield: 95.6%; Mp: 320 °C; ^{1}H NMR (500 MHz, dimethyl sulfoxide (DMSO)-d_6): δ 8.43 (d, 1H, $J = 2.0$ Hz), 8.26 (d, 1H, $J = 2.0$ Hz), 8.09 (d, 1H, $J = 2.0$ Hz), 8.08 (d, 1H, $J = 2.0$ Hz), 6.98 (s, 1H), 6.96 (s, 1H). ^{13}C-NMR (125 MHz, DMSO-d_6): δ 161.7, 153.2, 144.5, 140.3, 133.5, 128.6, 126.7, 126.7, 121.9, 119.4, 115.23, 115.2; HREI-MS: *m/z* calcd for $C_{12}H_8BrN_3O$ $[M]^+$ 288.9851; found 288.9847; anal. calcd for $C_{12}H_8BrN_3O$: C, 49.68; H, 2.78; N, 14.48; found: C, 49.66; H, 2.79; N, 14.47

*6-Bromo-2-(3,4-dimethoxyphenyl)-1*H-*imidazo[4,5-b] pyridine (**2**)*

Yield: 55.3%; Mp: 278 °C, ^{1}H NMR (500 MHz, DMSO-d_6): δ 8.35 (d, 1H, $J = 2.0$ Hz), 8.18 (s, 1H), 7.83 (s, 1H), 7.82 (s, 1H), 7.16 (d, 1H, $J = 8.5$ Hz), 3.88 (s, 3H, OCH3), 3.85 (s, 3H, OCH3). ^{13}C-NMR (125 MHz, DMSO-d_6): δ 155.8, 153.9, 150.4, 143.4, 139.4, 134.7, 128.6, 125.9, 121.9, 119.4, 114.2, 110.5, 57.7, 57.7; HREI-MS: *m/z* calcd for $C_{14}H_{12}BrN_3O_2$ $[M]^+$ 333.0113; found 333.0117; anal. calcd for $C_{14}H_{12}BrN_3O_2$: C, 50.32; H, 3.62; N, 12.57; found: C, 50.33; H, 3.64; N, 12.55

*6-Bromo-2-(4-methoxyphenyl)-1*H-*imidazo [4,5-b]pyridine (**3**)*

Yield: 73.3% ; Mp: 296 °C, ^{1}H NMR (500 MHz, DMSO-d_6): δ 13.60 (s, 1H, NH), 8.38 (s, 1H), 8.24 (s, 1H), 8.19 (d, 1H, $J = 8.5$ Hz), 7.15 (d, 1H, $J = 8.5$ Hz). ^{13}C-NMR (125 MHz, DMSO-d_6): δ 161.47, 152.34, 144.68, 140.23, 133.87, 127.56, 126.79, 126.79, 125.43, 118.34, 114.76, 114.76, 58.0; HREI-MS: *m/z* calcd for $C_{13}H_{10}BrN_3O$ $[M]^+$ 303.0007; found 303.0013; anal. calcd for $C_{13}H_{10}BrN_3O$: C, 51.34; H, 3.31; N, 13.82; found: C, 51.35; H, 3.30; N, 13.81

*2-(6-Bromo-1*H-*imidazo[4,5-b]pyridin-2-yl)benzene-1,4-diol (**4**)*

Yield: 96.6%; Mp: 353 °C; ^{1}H NMR (500 MHz, DMSO-d_6): δ 13.16 (s, 1H, NH), 9.17 (s, 1H), 8.46 (s, 1H), 7.52 (s,1H), 6.90 (s,1H). ^{13}C-NMR (125 MHz, DMSO-d_6): δ 153.6, 151.1, 150.4, 146.4, 140.3, 133.9, 127.5, 118.7, 117.4, 116.9, 115.2, 113.4; HREI-MS: *m/z* calcd for $C_{12}H_8BrN_3O_2$ $[M]^+$ 304.9800; found 304.9793; anal. calcd for $C_{12}H_8BrN_3O_2$: C, 47.08; H, 2.63; N, 13.73; found: C, 47.02; H, 2.65; N, 13.72

*6-Bromo-2-(4-chlorophenyl)-1*H-*imidazo[4,5-b]pyridine (**5**)*

Yield: 84.0%; Mp: 340 °C; ^{1}H NMR (500 MHz, DMSO-d_6): δ 834 (d, 1H, $J = 2.0$ Hz), 8.25 (d, 1H, $J = 8.5$ Hz), 8.18 (s, 1H), 6.72 (s, 1H). ^{13}C-NMR (125 MHz, DMSO-d_6): δ 154.2, 144.2, 141.4, 134.3, 133.5, 132.7, 129.2, 127.1, 126.3, 114.4; HREI-MS: *m/z* calcd for $C_{12}H_7BrClN_3$ $[M]^+$ 306.9512; found 306.9519; anal. calcd for $C_{12}H_7BrClN_3$: C, 46.71; H, 2.29; N, 13.62; found: C, 46.72; H, 2.31; N, 13.64

*6-Bromo-2-(pyridin-3-yl)-1*H-*imidazo[4,5-b]pyridine (**6**)*

Yield: 56.0%; Mp: 340 °C; ^{1}H NMR (500 MHz, DMSO-d_6): δ 8.75 (s, 1H), 8.74 (s, 1H), 8.56 (d, 1H, $J = 8.0$ Hz), 8.34 (s, 1H), 7.47 (d, 1H, $J = 2.0$ Hz), 7.65 (t, 1H). ^{13}C-NMR (125 MHz, DMSO-d_6): δ 154.2, 151.0, 148.8, 143.4, 139.4, 134.7, 132.7, 130.1, 129.0, 127.5, 118.9; HREI-MS: *m/z* calcd for $C_{11}H_7BrN_4$ $[M]^+$ 273.9854; found 273.9847; anal. calcd for $C_{11}H_7BrN_4$: C, 48.02; H, 2.56; N, 20.37; found: C, 48.01; H, 2.54; N, 20.38

*6-Bromo-2-p-tolyl-1*H-*imidazo[4,5-b]pyridine (**7**)*

Yield: 88.2%; Mp: 318 °C; ^{1}H NMR (500 MHz, DMSO-d_6): δ 8.39 (d, 1*H*, $J = 2.0$ Hz), 8.23 (d, 1H, $J = 2.0$ Hz), 8.13 (s, 1H), 8.12 (s, 1H), 7.39 (d, 1H, $J = 2.0$ Hz), 2.40 (s, 3H, CH3). ^{13}C-NMR (125 MHz, DMSO-d_6): δ 151.2, 143.4, 142.4, 137.7, 132.7, 130.2, 130.2, 128.7, 127.2, 127.2, 126.9, 119.4, 20.1; HREI-MS: *m/z* calcd for $C_{13}H_{10}BrN_3$ $[M]^+$ 287.0058; found 287.0064; anal. calcd for $C_{13}H_{10}BrN_3$: C, 54.19; H, 3.50; N, 14.58; found: C, 54.21; H, 3.51; N, 14.56

*6-Bromo-2-(2-fluorophenyl)-1*H*-imidazo[4,5-b] pyridine (**8**)*

Yield: 62.0%; Mp: 226 °C; ^{1}H NMR (500 MHz, DMSO-d_6): δ 8.46 (d, 1H, $J = 2.0$ Hz), 8.25 (s, 1H), 8.22 (t, 1H), 7.65–7.60 (m, 3H), 7.48–7.41 (m, H). ^{13}C-NMR (125 MHz, DMSO-d_6): δ 162.4 (d, $J = 262.3$ Hz), 147.0, 142.4, 139.4, 132.7, 130.3, 128.9, 127.4, 124.1, 118.9, 117.4, 114.5; HREI-MS: *m/z* calcd for $C_{12}H_7BrFN_3$ $[M]^+$ 290.9807; found 290.9801; anal. calcd for $C_{12}H_7BrFN_3$: C, 49.34; H, 2.42; N, 14.39; found: C, 49.35; H, 2.43; N, 14.37

*3-(6-Bromo-1*H*-imidazo[4,5-b]pyridin-2-yl)phenol (**9**)*

Yield: 67.0%; Mp: above 350 °C; ^{1}H NMR (500 MHz, DMSO-d_6): δ 8.43 (s, 1H), 8.27 (s, 1H), 7.66 (d, 1H, $J =$ 6.0 Hz), 7.38 (t.1H), 6.97 (d, 1H, $J = 8.5$ Hz). ^{13}C-NMR (125 MHz, DMSO-d_6): δ 158.7, 152.4, 144.7, 140.3, 133.8, 132.4, 130.6, 128.6, 118.0, 117.4, 116.1, 113.4; HREI-MS: *m/z* calcd for $C_{12}H_8BrN_3O$ $[M]^+$ 288.9851; found 288.9856; anal. calcd for $C_{12}H_8BrN_3O$: C, 49.68; H, 2.78; N, 14.48; found: C, 49.76; H, 2.77; N, 14.47

*5-(6-Bromo-1*H*-imidazo[4,5-b]pyridin-2-yl)-2-methoxyphenol (**10**)*

Yield: 56.0%; Mp: 276 °C; ^{1}H NMR (500 MHz, DMSO-d_6): δ 8.38 (d, 1H, $J = 1.5$ Hz), 8.20 (d, 1H, $J = 2.0$ Hz), 7.68 (s, 1H), 7.67 (d, 1H, $J = 2.0$ Hz), 7.13 (s, 1H), 7.11 (s, 1H), 3.87 (s, 3H, OCH3). ^{13}C-NMR (125 MHz, DMSO-d_6): δ 151.5, 149.3, 148.2, 145.4, 142.4, 132.7, 128.6, 123.8, 118.0, 117.2, 115.3, 109.3, 58.7; HREI-MS: *m/z* calcd for $C_{13}H_{10}BrN_3O_2$ $[M]^+$ 318.9956; found 318.9948; anal. calcdanal. calcd for $C_{13}H_{10}BrN_3O_2$: C, 48.77; H, 3.15; N, 13.13 found C, 48.78; H, 3.13; N, 13.12

*6-Bromo-2-(pyridin-4-yl)-1*H*-imidazo[4,5-b]pyridine (**11**)*

Yield: 80.7%; Mp: 336 °C, ^{1}H NMR (500 MHz, DMSO-d_6): δ 8.79 (s, 1H), 8.48 (d, 1H, $J = 2.0$ Hz), 8.36 (s, 1H), 8.14 (d, 1H, $J = 6.0$ Hz). ^{13}C-NMR (125 MHz, DMSO-d_6): δ 153.2, 151.4, 151.4, 143.4, 139.4, 140.8, 133.7, 128.6, 123.5, 123.5, 115.4; HREI-MS: *m/z* calcd for $C_{11}H_7BrN_4$ $[M]^+$ 273.9854; found 273.9861; anal. calcd for $C_{11}H_7BrN_4$: C, 48.02; H, 2.56; N, 20.37; found: C, 48.03; H, 2.54; N, 20.36

*4-(6-Bromo-1*H*-imidazo[4,5-b]pyridin-2-yl)benzene-1,2-diol (**12**)*

Yield: 97.0%; Mp: 350 °C, ^{1}H NMR (500 MHz, DMSO-d_6): δ 8.35 (d, 1H, $J = 2.0$ Hz), 8.16 (s, 1H), 7.90 (d, 1H, $J = 8.5$ Hz), 7.65 (s, 1H), 7.55 (s, 1H), 7.53 (d, 1H, $J = 2.0$ Hz). ^{13}C-NMR (125 MHz, DMSO-d_6): δ 152.4, 148.6, 145.4, 142.4, 135.7, 128.6, 120.6, 117.1, 116.4, 113.5, 111.1; HREI-MS: *m/z* calcd for $C_{12}H_8BrN_3O_2$ $[M]^+$ 304.9800; found 304.9808; anal. calcd for $C_{12}H_8BrN_3O_2$: C, 47.08; H, 2.63; N, 13.73; found: C, 47.06; H, 2.64; N, 13.71

*6-Bromo-2-o-tolyl-1*H*-imidazo[4,5-b]pyridine (**13**)*

Yield: 84.1%; Mp: 226 °C; ^{1}H NMR (500 MHz, DMSO-d_6): δ 8.44 (d, 1H, $J = 2.0$ Hz), 8.28 (d, 1H, $J = 2.0$ Hz), 7.80 (d, 1H, $J = 7.5$ Hz), 7.47–7.37(m, 3H), 2.61 (s, 3H, CH3). ^{13}C-NMR (125 MHz, DMSO-d_6): δ 149.2, 143.4, 139.4, 133.6, 132.8, 131.7, 130.2, 128.5, 127.1, 126.6, 125.1, 115.4, 22.2; HREI-MS: *m/z* calcd for $C_{13}H_{10}BrN_3$ $[M]^+$ 287.0058; found 287.0058; anal. calcd for $C_{13}H_{10}BrN_3$: C, 54.19; H, 3.50; N, 14.58; found: C, 54.18; H, 3.52; N, 14.57

*4-(6-Bromo-1*H*-imidazo[4,5-b]pyridin-2-yl)benzene-1,3-diol (**14**)*

Yield: 80.5%; Mp: above 350 °C; ^{1}H NMR (500 MHz, DMSO-d_6): δ 8.43 (d, 1H, $J = 2.0$ Hz), 8.26 (s,1H), 7.96 (d, 1H, $J = 8.5$ Hz), 6.49 (s, 1H), 6.47 (s, 1H), 6.44 (d, 1H, $J =$ 2.0 Hz). ^{13}C-NMR (125 MHz, DMSO-d_6): δ 164.6, 159.7, 153.2, 146.4, 140.6, 133.3, 129.5, 127.2, 118.7, 109.3, 104.8, 105.1; HREI-MS: *m/z* calcd for $C_{12}H_8BrN_3O_2$ $[M]^+$ 304.9800; found 304.9792; anal. calcd for $C_{12}H_8BrN_3O_2$: C, 47.08; H, 2.63; N, 13.73; found: C, 47.07; H, 2.64; N, 13.75.

*2-(6-Bromo-1*H*-imidazo[4,5-b]pyridin-2-yl)-4-methoxyphenol (**15**)*

Yield: 83.6%; Mp: 326 °C; ^{1}H NMR (500 MHz, DMSO-d_6): δ 13.30 (s, 1H, NH), 8.49 (s, 1H), 8.43 (s,1H), 8.25 (s,1H), 7.73 (d, 1H, $J = 3.0$ Hz), 7.08 (d, 1H, $J = 2.5$ Hz), 7.06 (d, 1H, $J = 2.5$ Hz), 7.01(s, 1H), 3.81 (s, 3H,OCH3). ^{13}C-NMR (125 MHz, DMSO-d_6): δ 155.7, 152.1, 150.2, 143.4, 139.4, 132.7, 128.6, 117.4, 116.1, 114.9, 113.6, 112.0, 55.0; HREI-MS: *m/z* calcd for $C_{13}H_{10}BrN_3O_2$ $[M]^+$ 318.9956; found 318.9965; anal. calcd for $C_{13}H_{10}BrN_3O_2$: C, 48.77; H, 3.15; N, 13.13; found C, 48.79; H, 3.16; N, 13.12

*6-Bromo-2-(furan-2-yl)-1*H*-imidazo[4,5-b]pyridine (**16**)*

Yield: 99.6%; Mp: 328 °C; ^{1}H NMR (500 MHz, DMSO-d_6): δ 8.41 (d, 1H, $J = 2.0$ Hz), 8.02 (d, 1H, $J = 1.0$ Hz), 7.36 (s, 1H), 7.35 (s, 1H), 6.79 (t.1H). ^{13}C-NMR (125 MHz, DMSO-d_6): δ 148.5, 148.8, 144.8, 144.0, 140.3, 133.7, 127.6, 118.4, 117.1, 112.0; HREI-MS: *m/z* calcd for

$C_{10}H_6BrN_3O$ $[M]^+$ 262.9694; found 262.9687; anal. calcd for $C_{10}H_6BrN_3O$: C, 45.48; H, 2.29; N, 15.91; found: C, 45.49; H, 2.28; N, 15.90

*6-Bromo-2-(3-methoxyphenyl)-1*H-*imidazo[4,5-b]pyridine* ***(17)***

Yield: 99.7%; Mp: 272 °C; ^{1}H NMR (500 MHz, DMSO-d_6): δ 13.76 (s, 1H, NH), 8.43 (s, 1H), 8.33 (s,1H), 7.84 (d, 1H, $J = 8.0$ Hz), 7.81 (s, 1H), 7.50 (t, 1H), 7.15 (d, 1H, $J =$ 2.0 Hz), 7.13 (d, 1H, $J = 2.0$ Hz), 3.88 (s, 3H,OCH3). ^{13}C-NMR (125 MHz, DMSO-d_6): δ 162.4, 151.9, 144.8, 140.3, 133.7, 131.6, 129.0, 127.6, 119.3, 118.4, 114.6, 114.0, 58.3; HREI-MS: *m/z* calcd for $C_{13}H_{10}BrN_3O$ $[M]^+$ 303.0007; found 303.0014; anal. calcd for $C_{13}H_{10}BrN_3O$: C, 51.34; H, 3.31; N, 13.82; found: C, 51.35; H, 3.33; N, 13.80

*3-(6-Bromo-1*H-*imidazo[4,5-b]pyridin-2-yl)benzene-1,2-diol* ***(18)***

Yield: 95.0%; Mp: 298 °C; ^{1}H NMR (500 MHz, DMSO-d_6): δ 8.48 (s, 1H), 8.43 (s, 1H), 7.58 (d, 1H, $J = 8.0$ Hz), 6.97 (d, 1H, $J = 7.5$ Hz), 6.85 (t, 1H). ^{13}C-NMR (125 MHz, DMSO-d_6): δ 153.5, 148.9, 146.6, 145.4, 142.3, 136.7, 124.6, 121.1, 119.5, 117.4, 115.1, 112.4 (s); HREI-MS: *m/z* calcd for $C_{12}H_8BrN_3O_2$ $[M]^+$ 304.9800; found 304.9809; anal. calcd for $C_{12}H_8BrN_3O_2$: C, 47.08; H, 2.63; N, 13.73; found: C, 47.07; H, 2.62; N, 13.75

*6-Bromo-2-m-tolyl-1*H-*imidazo[4,5-b]pyridine* ***(19)***

Yield: 68.7%; Mp: 292 °C; ^{1}H NMR (500 MHz, DMSO-d_6): δ 13.72 (s, 1H, NH), 8.40 (s, 1H), 8.08 (s, 1H), 8.03 (d, 1H, $J = 7.5$ Hz), 7.47 (t, 1H), 7.39 (d, 1H, $J = 7.5$ Hz), 2.43 (s, 3H,CH3). ^{13}C-NMR (125 MHz, DMSO-d_6): δ 152.9, 145.8, 141.4, 136.3, 135.7, 132.5, 130.1, 128.9, 127.6, 126.6, 124.0, 118.4, 21.0; HREI-MS: *m/z* calcd for $C_{13}H_{10}BrN_3$ $[M]^+$ 287.0058; found 287.0058; anal. calcd for $C_{13}H_{10}BrN_3$: C, 54.19; H, 3.50; N, 14.58 found: C, 54.19; H, 3.50; N, 14.58

*6-Bromo-2-(3-fluorophenyl)-1*H-*imidazo[4,5-b]pyridine* ***(20)***

Yield: 89.0%; Mp: 325 °C; ^{1}H NMR (500 MHz, DMSO-d_6): δ 13.89 (s, 1H, NH), 8.50 (s, 1H), 8.45(s, 1H), 8.39 (s, 1H), 8.23 (s, 1H), 8.11 (d, 1H, $J = 7.5$ Hz), 8.04 (d, 1H, $J =$ 2.0 Hz), 8.02 (d, 1H, $J = 2.0$ Hz), 7.67–7.63 (m, 3H), 7.44 (t, 1H). ^{13}C-NMR (125 MHz, DMSO-d_6): δ 164.6 (d, $J =$ 259.3 Hz), 152.9, 144.8, 141.4, 131.7, 130.5, 129.5, 127.6, 120.0, 119.4, 114.5, 114.3, 113.2; HREI-MS: *m/z* calcd for $C_{12}H_7BrFN_3$ $[M]^+$ 290.9807; found 290.9807; anal. calcd for $C_{12}H_7BrFN_3$: C, 49.34; H, 2.42; N, 14.39; found: C, 49.34; H, 2.42; N, 14.39

*6-Bromo-2-(2-nitrophenyl)-1*H-*imidazo[4,5-b]pyridine* ***(21)***

Yield: 48.2%; Mp: 216 °C; ^{1}H NMR (500 MHz, DMSO-d_6): δ 13.93 (s, 1H, NH), 8.12 (s, 1H), 8.10 (s, 1H), 8.01 (d, 1H, $J = 1.0$ Hz), 8.00 (d, 1H, $J = 1.5$ Hz), 7.93 (t, 1H), 7.85 (t, 1H). ^{13}C-NMR (125 MHz, DMSO-d_6): δ 150.7, 148.1, 144.2, 143.3, 135.2, 132.2, 130.3, 129.4, 128.0, 126.2, 124.3, 116.5; HREI-MS: *m/z* calcd for $C_{12}H_7BrN_4O_2$ $[M]^+$ 317.9752; found 317.9759; anal. calcd for $C_{12}H_7BrN_4O_2$: C, 45.17; H, 2.21; N, 17.56; found: C, 45.18; H, 2.19; N, 17.54

*6-Bromo-2-(thiophen-2-yl)-1*H-*imidazo[4,5-b]pyridine* ***(22)***

Yield: 89.0%; Mp: 310 °C; ^{1}H NMR (500 MHz, DMSO-d_6): δ 13.80 (s, 1H, NH), 7.98 (d, 1H, $J = 1.0$ Hz), 7.97(d, 1H, $J = 1.5$ Hz), 7.85 (s, 1H), 7.84 (s, 1H), 7.29 (t,1H). ^{13}C-NMR (125 MHz, DMSO-d_6): δ 148.1, 143.3, 140.4, 139.8, 130.4, 130.0, 127.5, 127.0, 126.3, 116.1; HREI-MS: *m/z* calcd for $C_{10}H_6BrN_3S$ $[M]^+$ 278.9466; found 278.9475; anal. calcd for $C_{10}H_6BrN_3S$: C, 42.87; H, 2.16; N, 15.00; found: C, 42.89; H, 2.15; N, 14.98

*2-(6-Bromo-1*H-*imidazo[4,5-b]pyridin-2-yl)phenol* ***(23)***

Yield: 85.0%; Mp: 318 °C; ^{1}H NMR (500 MHz, DMSO-d_6): δ 12.71 (s, 1H, NH), 8.50 (d, 1H, $J = 1.5$ Hz), 8.15 (d, 1H, $J = 8.5$ Hz), 7.38 (t, 1H), 7.04 (s, 1H). ^{13}C-NMR (125 MHz, DMSO-d_6): δ 158.9, 153.0, 148.1, 143.3, 131.0, 130.3, 129.8, 126.3, 121.0, 118.4, 116.1, 111.7; HREI-MS: *m/z* calcd for $C_{12}H_8BrN_3O$ $[M]^+$ 288.9851; found 288.9859; anal. calcd for $C_{12}H_8BrN_3O$: C, 49.68; H, 2.78; N, 14.48; found: C, 49.69; H, 2.76; N, 14.46

*2-(6-Bromo-1*H-*imidazo[4,5-b]pyridin-2-yl)-5-methoxyphenol* ***(24)***

Yield: 87.5%; Mp: 314 °C; ^{1}H NMR (500 MHz, DMSO-d_6): δ 12.90 (s, 1H, NH), 8.42 (d, 1H, $J = 2.0$ Hz), 8.33 (s, 1H), 8.04 (s, 1H), 8.02 (s, 1H), 8.66 (d, 1H, $J = 2.0$ Hz), 8.65 (d, 1H, $J = 2.5$ Hz), 8.61 (d, 1H, $J = 2.5$ Hz). ^{13}C-NMR (125 MHz, DMSO-d_6): δ 160.6, 160.3, 153.9, 148.1, 143.5, 130.3, 130.6, 126.2, 116.5, 108.0, 107.6, 102.1, 56.0; HREI-MS: *m/z* calcd for $C_{13}H_{10}BrN_3O_2$ $[M]^+$ 318.9956; found 318.9962; anal. calcd for $C_{13}H_{10}BrN_3O_2$: C, 48.77; H, 3.15; N, 13.13; found: C, 48.78; H, 3.14; N, 13.14

*6-Bromo-2-(2-chlorophenyl)-1H-imidazo[4,5-b]pyridine (**25**)*

Yield: 61.0%; Mp: 239 °C; ^{1}H NMR (500 MHz, DMSO-d_6): δ 13.64 (s, 1H, NH), 7.88 (s, 1H), 7.70 (s, 1H), 7.68 (d, 1H, $J = 1.0$ Hz), 7.62 (t, 1H), 7.55 (t, 1H). ^{13}C-NMR (125 MHz, DMSO-d_6): δ 148.1, 144.3, 143.3, 132.1, 131.7, 130.6, 130.0, 130.3, 128.8, 127.8, 126.2, 116.5; HREI-MS: *m/z* calcd for $C_{12}H_7BrClN_3$ $[M]^+$ 306.9512; found 306.9521; anal. calcd for $C_{12}H_7BrClN_3$: C, 46.71; H, 2.29; N, 13.62; found: C, 46.73; H, 2.27; N, 13.63

*6-Bromo-2-(3-chlorophenyl)-1H-imidazo[4,5-b]pyridine (**26**)*

Yield: 86.7%; Mp: 330 °C; ^{1}H NMR (500 MHz, DMSO-d_6): δ 13.79 (s, 1H, NH), 8.46 (d, 1H, $J = 2.0$ Hz), 8.33 (s, 1H), 8.28 (s, 1H), 8.21–8.19 (m, 3H), 7.65–7.63 (m, 3H), 7.61 (s, 1H). ^{13}C-NMR (125 MHz, DMSO-d_6): δ 148.1, 144.3, 143.3, 132.1, 131.7, 130.6, 130.0, 130.3, 128.8, 127.8, 126.2, 116.5; HREI-MS: *m/z* calcd for $C_{12}H_7BrClN_3$ $[M]^+$ 306.9512; found 306.9508; anal. calcd for $C_{12}H_7BrClN_3$: C, 46.71; H, 2.29; N, 13.62; found: C, 46.72; H, 2.30; N, 13.60

*6-Bromo-2-(3-nitrophenyl)-1H-imidazo[4,5-b]pyridine (**27**)*

Yield: 82.0%; Mp: 324 °C; ^{1}H NMR (500 MHz, DMSO-d_6): δ 9.07 (d, 1H, $J = 1.5$ Hz), 8.66 (d, 1H, $J = 7.5$ Hz), 8.45 (d, 1H, $J = 2.0$ Hz), 8.38 (s, 1H), 8.37 (s, 1H), 8.32 (s, 1H), 7.89 (t, 1H). ^{13}C-NMR (125 MHz, DMSO-d_6): δ 150.7, 148.1, 144.1, 143.3, 135.4, 132.3, 130.3, 129.4, 128.0, 126.2, 124.3, 115.1; HREI-MS: *m/z* calcd for $C_{12}H_7BrN_4O_2$ $[M]^+$ 317.9752; found 317.9758; anal. calcd for $C_{12}H_7BrN_4O_2$: C, 45.17; H, 2.21; N, 17.56; found: C, 45.18; H, 2.20; N, 17.54

*6-Bromo-2-(pyridin-2-yl)-1H-imidazo[4,5-b]pyridine (**28**)*

Yield: 60.7%; Mp: 318 °C; ^{1}H NMR (500 MHz, DMSO-d_6): δ 8.78 (t, 1H), 8.47 (d, 1H, $J = 2.0$ Hz), 8.38 (s, 1H), 8.36 (d, 1H, $J = 1.5$ Hz), 8.22 (s, 1H), 8.06–8.03 (m, 3H), 7.60–7.58 (m, 3H). ^{13}C-NMR (125 MHz, DMSO-d_6): δ 149.41, 148.11, 147.20, 143.37, 143.09, 141.77, 130.43, 126.61, 126.23, 124.38, 116.51; HREI-MS: *m/z* calcd for $C_{11}H_7BrN_4$ $[M]^+$ 273.9854; found 273.9861; anal. calcd for $C_{11}H_7BrN_4$: C, 48.02; H, 2.56; N, 20.37; found: C, 48.03; H, 2.57; N, 20.36

*6-Bromo-2-(4-fluorophenyl)-1H-imidazo[4,5-b]pyridine (**29**)*

Yield: 92.7%; Mp: 336 °C; ^{1}H NMR (500 MHz, DMSO-d_6): δ 13.70 (s, 1H, NH), 8.43 (s, 1H), 8.30–8.27 (m, 3H), 7.47 (t, 1H). ^{13}C-NMR (125 MHz, DMSO-d_6): δ 165.8 (d, $J = 264.3$ Hz), 148.7, 148.1, 143.3, 130.4, 129.8, 129.8, 126.3, 116.5, 116.5, 116.1, 115.5; HREI-MS: *m/z* calcd for $C_{12}H_7BrFN_3$ $[M]^+$ 290.9807; found 290.9813; anal. calcd for $C_{12}H_7BrFN_3$: C, 49.34; H, 2.42; N, 14.39; found: C, 49.35; H, 2.43; N, 14.38

α-Glucosidase inhibition assay

The α-glucosidase inhibition assay had been carried out using Baker's yeast α-glucosidase (EC 3.2.1.20) and *p*-nitrophenyl-α-D-glucopyranoside. The samples (5 µg ml^{-1}) were prepared by dissolving the compounds (**3–32**) in DMSO. Test samples (10 µL), which had been prepared, were reconstituted in 100 µL of phosphate buffer (100 mM) at pH 6.8 in 96-well micro-plate and incubated with 50 µL of Baker's yeast α-glucosidase for 5 min before 50 µL of *p*-nitrophenyl-α-D-glucopyranoside (5 mM) was added. After incubating for 5 min, the absorbance was measured at 405 nm using SpectraMax plus384 (Molecular Devices Corporation, Sunnyvale, CA, USA). Blank in which the substrate was replaced with 50 µL of buffer were analyzed to accurately determine the background absorbance. Positive control samples (acarbose and voglibase) were prepared to contain 10 µL DMSO instead of test samples.

Pharmacokinetic predictions of the phenyl-imidazo-pyridine derivatives

In silico pharmacokinetic and absorption distribution metabolism excretion properties were evaluated for the phenyl-imidazo-pyridine derivatives using the QikProp program (Duffy and Jorgensen 2000), implemented in Maestro [Maestro, Version 9.2, Schrodinger, LLC, New York, NY, USA, 2011]. Prior to QikProp, the derivatives were neutralized using ligprep module of Maestro. Principally, four descriptors were taken into account for assessment: Lipinski's rule of five is a rule of thumb to assess drug likeness (Lipinski et al. 1997), the predicted aqueous solubility (QP log *S*), the predicted octanol/water partition coefficient (QP log*P*) and the predicted Caco-2 cell permeability (QPPcaco).

Molecular docking studies

Glide docking (Schrödinger 2015), a program for complete solution for ligand–receptor docking in small molecule drug discovery suite, was employed to identify the binding modes of the 30 phenyl-imidazo-pyridine derivatives (**3–32**) accountable for the activity. The α-glucosidase protein structure (pdb id: 3top) was used in the study and acarbose. The reference molecular binding site was considered as center with 12 Å radius for grid box generation. The standard precision (SP) mode was selected as preferred mode

Scheme 1 Synthesis of 2-phenyl-1*H*-imidazo[4,5-*b*] pyridines (**3–32**)

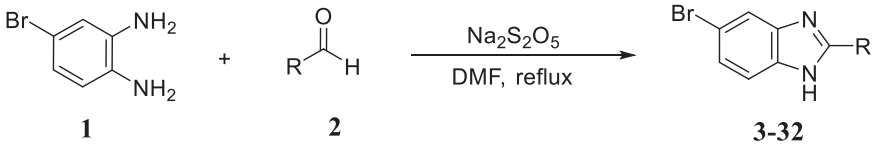

during the Glide docking process and Glide gscore was taken into account for analysis. While, GOLD (Genetic Optimization for Ligand Docking) version 5.1 (Verdonk et al. 2003) was considered as docking validation program. Gold scoring fitness function was chosen. The genetic algorithm was set with search efficiency of 100%. The acarbose inhibition site on α-glucosidase protein structure (pdb id: 3TOP) with a cavity of 12 A° radius defined as active site. The results divergent by less than 1.5 Å in ligand all atom root-mean-square deviations were clustered collectively. Pymol (Pymol 2010), and Maestro visualization were used to analyze the best clusters and top rank scored binding mode.

Results and discussion

Chemistry

The synthetic route towards derivatives **3–32** is shown in Scheme 1. The starting material, 5-bromopyridine-2,3-diamine **1**, was treated with various substituted aromatic aldehyde metabisulfite adducts to form compounds **3–32**. The structures of derivatives **3–32** were confirmed using spectroscopic techniques such as NMR, MS and were further confirmed using CHN analysis.

α-Glucosidase inhibition

In our ongoing efforts of identifying new α-glucosidase inhibitors (Imran et al. 2015b, 2015c; Taha et al. 2015c), derivatives of imidazo[4,5-*b*]pyridine (**3–32**) were evaluated for their ability to inhibit Baker's yeast α-glucosidase. The IC_{50} values for all compounds were in the range of 13.5–93.7 µM (Table 1). The in vitro activities of the derivatives were compared with the IC_{50} value of acarbose ($IC_{50} = 38.25 \pm 0.12$ µM) and voglibase ($IC_{50} = 23.40 \pm 0.10$ μM); the standard inhibitors. Compound **15**, a 2,4-dihydroxy-substituted derivative displayed the most potent activity with an IC_{50} value of 13.5 ± 0.15 µM. Besides compound **15**, other compounds that were found to be active also include compounds **6** ($IC_{50} = 19.9 \pm 0.2$ µM), **7** ($IC_{50} = 29.4 \pm 0.3$ µM), **17** ($IC_{50} = 23.7 \pm 0.3$ µM), **21** ($IC_{50} = 19.4 \pm 0.2$ µM), **26** ($IC_{50} = 21.2 \pm 0.2$ µM), **27** ($IC_{50} = 23.5 \pm 0.2$ µM) and **31** ($IC_{50} = 33.3 \pm 0.3$ µM).

General observation suggests that the inhibitory potential of these derivatives is highly dependent upon the presence of hydroxy substitutions at different position of aromatic side chain. Based on structure activity relationship, it was observed that presence of hydroxyl group on the aromatic side chain significantly enhanced the inhibitory potential of certain derivatives against α-glucosidase enzyme. These findings suggest that presence of hydroxyl groups at a particular position is pertinent for compounds to be active against *a*-glucosidase. In the current series, observation on IC_{50} values in Table 1 shows that compounds having hydroxyl substituent at *ortho* and *para* positions are able to efficiently inhibit α-glucosidase enzyme.

The importance of hydroxyl at *ortho* and *para* positions can be evidently observed from the activity trend. Comparison between compounds **15** and **12** revealed that transformation of *para*-hydroxy substituent to methoxy causes a significant decrease in the inhibition potential. Comparison between the activities of these compounds also showed that *meta*-substituted hydroxyl group is not contributing significantly towards that activity. On the other hand, comparison between IC_{50} values of compounds **17** and **27** is suggestive of that hydroxyl group at *para* position is not as significant as hydroxyl group at *ortho* position is. The results for these compounds showed that replacing hydroxyl at *para* position with a methoxy group does not affect the activity significantly. The significant contribution of hydroxyl group at *ortho* position can also be observed through the results displayed by compounds **6** and **21**. It was observed for these two derivatives, besides the *ortho*-substituted hydroxyl group, additional hydroxyl group at other position does not show much affect on the IC_{50} values. This also confirms and strengthens the earlier hypothesis that hydroxyl group at *meta* position is less likely to play any significant role in the inhibitory potential of α-glucosidase enzyme. However, observation on activity of compound **18** suggests that hydroxyl at position C-5 for compound **6** is quite important as any attempt to replace this hydroxyl group reduces the activity significantly as being observed for compound **18**.

The phenyl-imidazo-pyridine derivatives and their four pharmacokinetic descriptor properties were analyzed by QikProp program, which consists of predicted Lipinski's rule-of-five, the predicted octanol/water partition coefficient (QP logP), predicted aqueous solubility (QP log *S*) and the predicted Caco-2 cell permeability (QPPcaco) and their results were listed in Table 1. Based on the results displayed in Table 1, all of the pharmacokinetic parameters of phenyl-imidazo-pyridine derivatives were within the acceptable

Table 1 Synthesis of imidazo[4,5-*b*]pyridines **3–32**

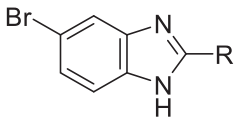

3-32

No.	R	No.	R
3	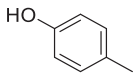	**18**	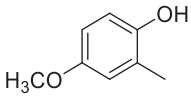
4	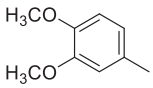	**19**	
5	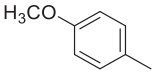	**20**	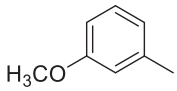
6	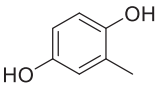	**21**	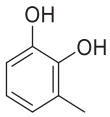
7	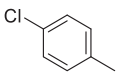	**22**	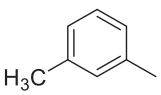
8		**23**	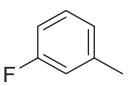
9	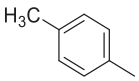	**24**	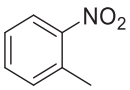
10	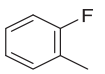	**25**	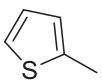
11	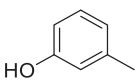	**26**	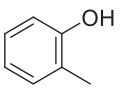
12	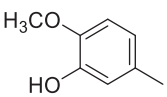	**27**	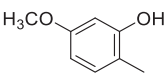
13	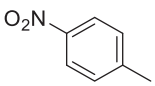	**28**	
14		**29**	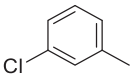

Table 1 continued

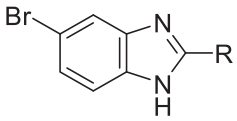

3-32

No.	R	No.	R
15	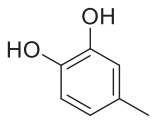	**30**	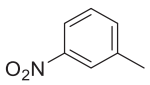
16	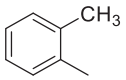	**31**	
17	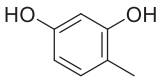	**32**	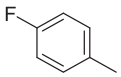

range for drug-likeness. These compounds possess that desired molecular properties in drug's pharmacokinetics in the human bodies that are crucial for being a perfect drug candidate.

Molecular docking studies were performed in order to better understand the inhibition mechanism of active compounds and to further establish the interaction of hydroxyl at different position towards the active site of α-glucosidase enzyme. The compounds were docked into the binding pocket of α -glucosidase enzyme to further confirm the inhibition potential and also the docked Glide gscore was reported for newly synthesized **3–32** compounds (Table 1).

Docking study

Glide docking tool was used for the protein–ligand interaction study. The phenyl-imidazo-pyridine derivatives along with the acarbose were docked using Glide (Glide gscore is shown in Table 1) targeting the human intestinal α-glucosidase C-terminal domain. Flexibility of the ligand was taken into consideration to predict the correct conformation and to obtain minimum energy structures. The top ranked pose of each molecule was chosen on the basis of docking score (S) for further analysis. The results were analyzed considering the best binding mode in glide docking program and each compound's binding mode agreement with the GOLD docking. The best binding mode of each compound were considered for interaction pattern (H-bonding, hydrophobic and π–π interactions). Our analysis showed that the active molecules of the

Table 2 In vitro α-glucosidase inhibition activity of derivatives **3–32** and their predicted pharmacokinetic properties

Compound	Lipinski's rule of five[a]	QPlog $P_{o/w}$[b]	QPlog S[c]	QP P_{caco}[d] [nm s^{-1}]	Glide gscore[e]	IC_{50} (μM ± SEM[a])
3	0	2.316	−3.723	784.35	−5.404	39.60 ± 0.39
4	0	3.335	−4.567	2584.794	−5.061	N. A.
5	0	3.176	−4.258	2586.619	−5.064	N. A.
6	0	1.685	−3.397	346.775	−6.282	19.90 ± 0.19
7	0	3.559	−4.752	2588.832	−5.504	29.40 ± 0.28
8	0	2.161	−3.505	1395.823	−4.777	N. A.
9	0	3.375	−4.585	2588.557	−5.159	N. A.
10	0	3.307	−4.25	2830.205	−5.244	43.40 ± 0.49
11	0	2.317	−3.723	786.896	−5.216	93.70 ± 0.96
12	0	2.47	−4.001	849.941	−5.218	N. A.
13	0	2.287	−4.197	309.016	−4.454	N. A.
14	0	2.161	−3.506	1395.594	−4.834	N. A.
15	0	1.627	−3.434	283.907	−6.655	13.50 ± 0.15
16	0	3.357	−4.466	2655.38	−5.142	N. A.
17	0	1.785	−4.176	179.01	−6.058	23.70 ± 0.25
18	0	2.505	−3.945	986.481	−5.464	46.60 ± 0.45
19	0	2.347	−3.241	2181.849	−5.753	63.40 ± 0.65
20	0	3.168	−4.231	2589.198	−5.135	N. A.
21	0	1.746	−3.375	420.069	−6.563	19.40 ± 0.20
22	0	3.375	−4.586	2589.771	−5.278	N. A.
23	0	3.332	−4.376	2589.144	−5.152	N. A.
24	0	2.355	−4.141	418.67	−5.319	59.60 ± 0.60
25	0	2.961	−3.958	2412.615	−5.325	79.40 ± 0.80
26	0	2.423	−3.665	1140.025	−6.055	21.20 ± 0.21
27	0	2.536	−3.896	1142.428	−5.824	23.50 ± 0.23
28	0	3.501	3.501	2572.037	−5.455	39.40 ± 0.36
29	0	3.558	−4.75	2589.319	−5.133	N. A.
30	0	2.297	−4.219	310.445	−5.286	N. A.
31	0	2.441	−3.916	1668.021	−5.532	33.30 ± 0.33
32	0	3.333	−4.376	2588.969	−5.517	36.30 ± 0.37
Acarbose	0	−7.274	0.716	0.044	−7.388	**38.25 ± 0.12**
voglibase	1	−2.839	0.308	8.911	−8.511	**23.40 ± 0.10**

[a] Predicted rule of five: range of recommended values is maximum number 4

[b] Predicted octanol/water partition coefficient (QP log $P_{o/w}$): range of recommended values = −2.0− + 6.5

[c] Predicted aqueous solubility (QP log *S*): values less than −6 or greater than −1 are undesirable

[d] Predicted apparent Caco-2 cell permeability (QP P_{caco}): value < 25 is poor

[e] Predicted Glide gscore from Glide docking using SP mode

[f] *N.A* no activity

phenyl-imidazo-pyridine derivatives displayed substantial binding within the acarbose inhibition site i.e. active site of α-glucosidase (Table 2).

There was clear demarcation among the active and inactive derivatives in terms of the docked Glide gscore. The presence of the hydroxyl group at *ortho*, *meta* and *para* position on the phenyl ring of the phenyl-imidazo-pyridine derivatives shows activity. The four active most compounds are compound **14** (13.5 ± 0.2 μM/gscore: −6.655), compound **21** (19.4 ± 0.2 μM/gscore: −6.563), compound **6** (19.9 ± 0.2 μM/gscore:−6.282), and compound **26** (21.2 ± 0.2 μM/gscore: −6.055). In the case of inactive compounds, presence of hydrophobic groups on the phenyl ring, more specifically presence of methoxy group, will result in the loss of activity profile (compounds **4**, **5**, **9**, **12**, **17**, **21** and **23**). On the other hand the presence of halogen such as Cl or F at the *ortho*/*para* position of the phenyl-imidazo-pyridine derivatives displayed inhibitory activity (compounds **7** and **10**).

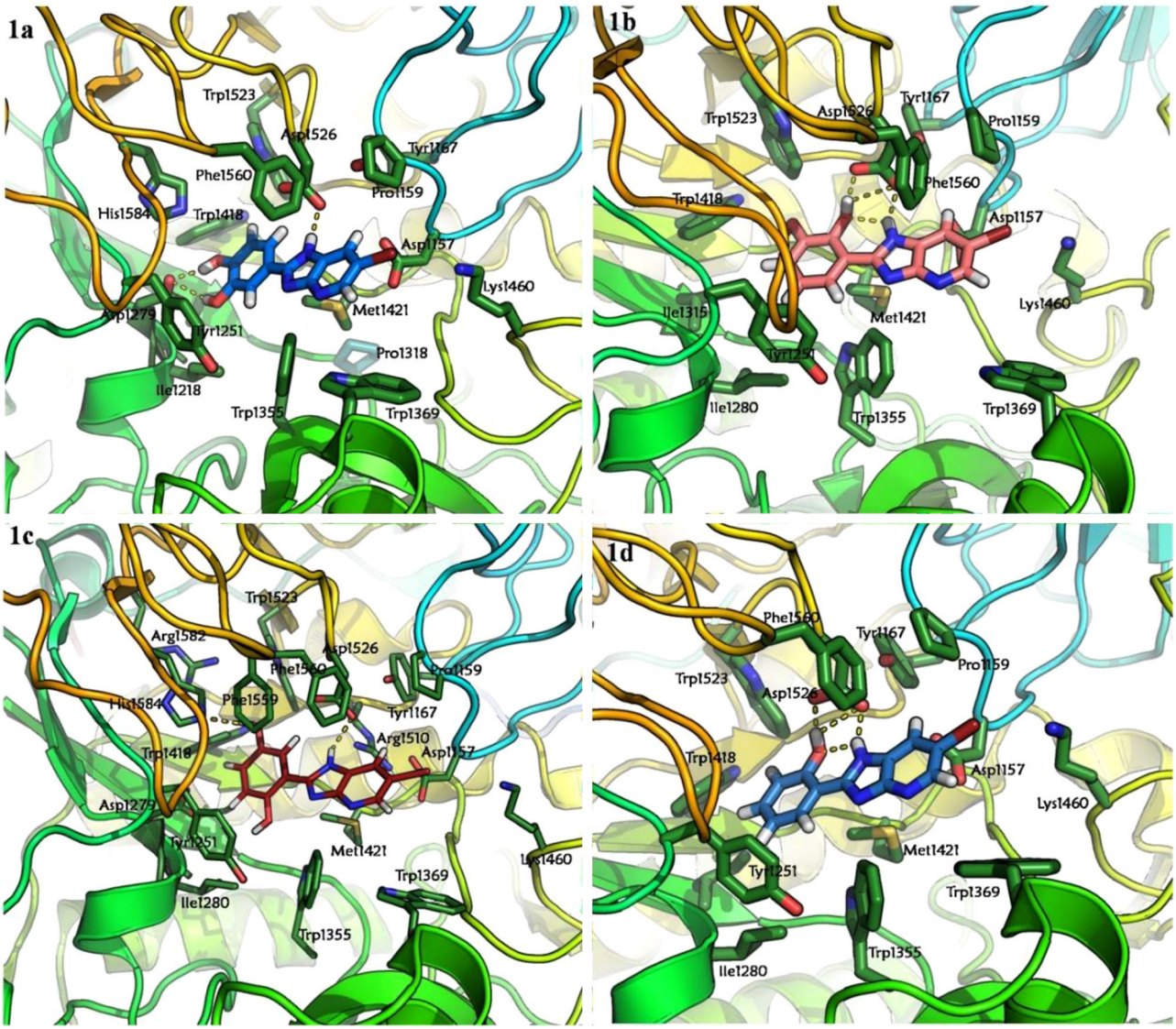

Fig. 2 Illustration of predicted binding mode of bromo phenyl-imidazo-pyridine derivatives in the binding site of α-glucosidase. **a**. Compound **15** (*blue color*) **b**. Compound **21** (*pink color*), **c**. Compound **6** (*brown color*), **d**. Compound **27** (*light blue color*). Key residues and compounds are shown stick and the H-bond interactions are represented in *yellow dashed lines*

Binding mode of the four most active compounds have been discussed much in detail. The most active among the series is compound **15**. The imidazo-pyridine NH formed H-bond with Asp1526, while the both the hydroxyl group of the catechol formed H-bond with Asp1279. Phe1560 formed π–π stacking with the imidazo-pyridine ring. Additionally the compounds are also stabilized by hydrophobic interactions of the imidazo-pyridine ring with the side chain of Pro1159, Tyr1167, Asp1157, Met1421, Trp1369, Pro1318, and Lys1460. Likewise the catechol ring forms hydrophobic interaction with Phe1560, Trp1523, Trp1418, His1584, Try1251, Ile1218 and Trp1355 (Fig. 1a).

The second most active molecule in the series was compound **21** that is shown in Fig. 2b. Asp1526 residue formed H-bond with both imidazo-pyridine NH and with hydroxyl group of catechol. Hydrophobic interaction is formed between bromoimidazo pyridine ring and side chains of Asp1157, Pro1159, Lys1460, Trp1369, Phe1560 and Trp1355. While the benzene ring of catechol moiety formed hydrophobic interactions with side chains of Met1421, Arg1510, Tyr1167, Trp1523, Trp1418, Ile1315, Tyr1251, Ile1280 and Trp1355.

The binding mode of the compound **6** as in Fig. 2c showed that one of the hydroxyl group of the α-hydroquinone forms H-bond with NH of the imidazole ring of

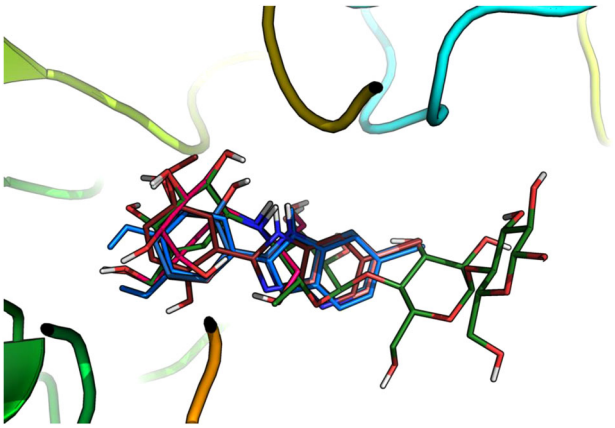

Fig. 3 The comparison of the binding mode of acarbose (*forest green color stick*) and voglibase (*hot pink color stick*) along with the four most potent compound's binding mode represented with same color code as in Fig. 1

His1584. Additionally, the benzene ring of catechol moiety forms hydrophobic interactions with side chains of Arg1510, Phe1559, Trp1523, Trp1418, Arg1582, Asp1526, Asp1279, Tyr1251, Ile1280 and Trp1355. While the imidazo-pyridine ring with the side chain of Met1421, Phe1560, Tyr1167, Lys1460, Asp1157, Pro1159 and Trp1369.

Figure 2d shows the interaction of the compound **26** revealing its binding mode. Asp1526 being the key residue forms H-bond with phenol OH and with imidazo-pyridine NH. While the bromo group forms hydrophobic interaction with Pro1159 and Lys1460, whereas bromoimidazo pyridine ring forms hydrophobic interaction with Trp1369, Phe1560 and Asp1157. Likewise the phenol ring forms hydrophobic interaction with Met1421, Tyr1167, Trp1418, Tyr1251, Ile1280, Trp1523 and Trp1355.

Analyzing both α-glucosidase inhibition data and the molecular interaction study clearly suggests that the hydroxyls attached to the phenyl ring of the phenyl-imidazo-pyridine derivatives are responsible for the activity, while the presence of hydrophilic group over the phenyl ring was accountable for the loss of activity. Alternatively presence of halogen at the *ortho*/*para* position was also showing activity and the presence of methoxy group over the ring decreases the activity index considerably.

Comparison of the binding mode of the acarbose and voglibase (anti-diabetic drug) between the four most potent compound at the active site of α-glucosidase showed that the phenyl ring of phenyl-imidazo-pyridine derivatives are exactly positioned in the same orientation to that of the cyclohexene and cyclohexane position of acarbose and voglibase, respectively. Likewise, potent derivatives have their imidazopyridine rings of the phenyl-imidazo-pyridine positioned exactly in similar orientation with one of the cyclic hexane as shown in Fig. 3. Therefore the predicted binding mode of the phenyl-imidazo-pyridine potent derivatives shows close binding mode orientation similarity to that of acarbose and voglibase. Hence this series of derivatives could be a good future drug candidate equivalent to that of well-known anti-diabetic drug such as acarbose and voglibase.

Consequently, the binding mode analysis of active compounds of the phenyl-imidazo-pyridine derivatives in the active site of α-glucosidase is facilitated by stable hydrogen bond network with the key residues in the active site. Addition, the hydrophobic interactions also significantly contribute for the stability of the interaction.

Conclusions

In conclusion, new compounds possessing imidazo[4,5-*b*] pyridine have been synthesized and identified as potent α-glucosidase inhibitor. The inhibitory results are well supported by structure-activity relationship, pharmacokinetic prediction and docking studies. Structure–activity relationship revealed that inhibitory potentials for derivatives **3–32** were dependent on presence of hydroxyl substituents at different positions of aromatic side chain, especially at *ortho*-positions and *para*-positions. Molecular docking analysis clearly demonstrated that binding mode of active compounds of the phenyl-imidazo-pyridine derivatives in the active site of α-glucosidase is facilitated by stable hydrogen bond network with the key residues in the active site. Additionally, the hydrophobic interactions also significantly contributed for the stability of the interactions. Pharmacokinetic parameters predicted for imidazo[4,5-*b*] pyridine derivatives were within the acceptable range for drug-likeness and it suggests that these compounds can potentially be the plausible drug candidates.

Acknowledgements Dr. Muhammad Taha would like to acknowledge the Ministry of Higher Education for financial support under the Fundamental Research Grant Scheme (FRGS) with sponsorship reference numbers FRGS/1/2016/STG01/UiTM/02/2 and Universiti Teknologi MARA for the financial support under LESTARI grant 600-RMI/DANA /5/3/ lestari (54/2013). The author (Dr. M.A.) is also grateful to HEC Pakistan for providing a research grant vide 20-1933/NRPU/R&D/HEC/12/5017.

Compliance with ethical standards

Conflict of interest The authors declare that they have no competing interest.

References

Adisakwattana S, Sookkongwaree K, Roengsumran S, Petsom A, Ngamrojnavanich N, Chavasiri W, Deesamer S, Yibchok-anun S (2004) Structure–activity relationships of trans-cinnamic acid

derivatives on α-glucosidase inhibition. Bioorg Med Chem Lett 14:2893–2896
Asano N, Oseki K, Tomioka E, Kizu H, Matsui K (1994) N-containing sugars from Morus alba and their glycosidase inhibitory activities. Carbohydr Res 259:243–255
Brownson C, Hipkiss A (2000) Carnosine reacts with a glycated protein. Free Radic Biol Med 28:1564–1570
Bukowski L, Kaliszan R (1991) Imidazo [4, 5-b] pyridine derivatives of potential tuberculostatic activity, II: synthesis and bioactivity of designed and some other 2-cyanomethylimidazo [4, 5-b] pyridine derivatives. Arch Pharm 324:537–542
Butler AE, Janson J, Bonner-Weir S, Ritzel R, Rizza RA, Butler PC (2003) Beta-cell deficit and increased beta-cell apoptosis in humans with type 2 diabetes. Diabetes 52:102–110
Charron MJ, Dubin RA, Michels CA (1986) Structural and functional analysis of the MAL1 locus of Saccharomyces cerevisiae. Mol Cell Biol 6:3891–3899
Chen YG, Li P, Li P, Yan R, Zhang XQ, Wang Y, Zhang XT, Ye WC, Zhang QW (2013) α-Glucosidase inhibitory effect and simultaneous quantification of three major flavonoid glycosides in Microctis folium. Molecules 18:4221–4232
Clark RL, Pessolano AA, Shen TY, Jacobus DP, Jones H, Lotti VJ, Flataker LM (1978) Synthesis and analgesic activity of 1, 3-dihydro-3-(substituted phenyl) imidazo [4, 5-b] pyridin-2-ones and 3-(substituted phenyl)-1, 2, 3-triazolo [4, 5-b] pyridines. J Med Chem 2:965–978
Danaei G, Finucane MM, Lu Y, Singh GM, Cowan MJ, Paciorek CJ, Lin JK, Farzadfar F, Khang YH, Stevens GA, Rao M, Ali MK, Riley LM, Robinson CA, Ezzati M (2011) Global burden of metabolic risk factors of chronic diseases collaborating group (blood glucose). Lancet 378:31–40
Duffy EM, Jorgensen WL (2000) Prediction of properties from simulations: free energies of solvation in hexadecane, octanol, and water. J Am Chem 122:2878–2888
Hsiao SH, Liao LH, Cheng PN, Wu TJ (2006) Hepatotoxicity associated with acarbose therapy. Ann Pharmacother 40:151–154
Hollander P (1992) Safety profile of acarbose, an α-glucosidase inhibitor. Drugs 44:47–53
Humphries MJ, Matsumoto K, White SL, Olden K (1986) Inhibition of experimental metastasis by castanospermine in mice: blockage of two distinct stages of tumor colonization by oligosaccharide processing inhibitors. Cancer Res 46:5215–5222
Imran S, Taha M, Ismail NH, Fayyaz S, Khan KM, Choudhary MI (2015a) Synthesis, biological evaluation, and docking studies of novel thiourea derivatives of bisindolylmethane as carbonic anhydrase II inhibitor. Bioorg Chem 62:83–93
Imran S, Taha M, Ismail NH, Kashif SM, Rahim F, Jamil W, Hariono M, Yusuf M, Wahab H (2015b) Synthesis of novel flavone hydrazones: in-vitro evaluation of α-glucosidase inhibition, QSAR analysis and docking studies. Eur J Med Chem 105:156–170
Imran S, Taha M, Ismail NH, Kashif SM, Rahim F, Jamil W, Wahab H, Khan KM (2015c) Synthesis, in vitro and docking studies of new flavone ethers as α-glucosidase inhibitors. Chem Biol Drug Des 87:361–373
Kumar S, Narwal S, Kumar V, Prakash O (2011) α-glucosidase inhibitors from plants: a natural approach to treat diabetes. Pharmacogn Rev 5:19–29
Lavanya P, Suresh M, Kotaiah Y, Harikrishna N, Rao CV (2011) Synthesis, antibacterial, antifungal and antioxidant activity studies on 6-bromo-2-substitutedphenyl-1H-imidazo [4, 5-b] pyridine. Asian J Pharm Clin Res 4:69–73
Lefebvre P, Scheen A (1994) The use of acarbose in the prevention and treatment of hypoglycaemia. Eur J Clin Invest 24:40–44
Lipinski CA, Lombardo F, Dominy BW, Feeney PJ (1997) Experimental and computational approaches to estimate solubility and permeability in drug discovery and development settings. Adv Drug Deliver Rev 23:3–25
Loriga M, Paglietti G, Piras S, Sparatore F, Anania V, Demontis MP, Varoni MV, Fattaccio MC (1992) Synthesis and evaluation of gastroprotective and antiulcer activity of some 2-substituted-1H-imidazo [4, 5-b] pyridines and-1H-benzimidazoles. Farmaco 47:287–303
Luo H, Imoto T, Hiji Y, World J (2001) Inhibitory effect of voglibose and gymnemic acid on maltose absorption in vivo. World J Gastroenterol 7:270–274
Mallemula VR, Sanghai NN, Himabindu V, Chakravarthy AK (2013) Synthesis and characterization of antibacterial 2-(pyridin-3-yl)-1H-benzo [d] imidazoles and 2-(pyridin-3-yl)-3H-imidazo [4, 5-b] pyridine derivatives. Res Chem Intermed 4:2125–2138
Matsuo T, Odaka H, Ikeda H, Am (1992) Effect of an intestinal disaccharidase inhibitor (AO-128) on obesity and diabetes. J Clin Nutr 55:314S–317S
Narasimhan B, Sharma D, Kumar P (2011) Biological importance of imidazole nucleus in the new millennium. Med Chem Res 20:1119–1140
NY L, Molecular Graphics System USA (2010) PyMOL New York, US
O'Dea K, Turton J (1985) Optimum effectiveness of intestinal alpha-glucosidase inhibitors: importance of uniform distribution through a meal. Am J Clin Nutr 41:511–516
Park H, Hwang KY, Oh KH, Kim YH, Lee JY, Kim K (2008) Discovery of novel α-glucosidase inhibitors based on the virtual screening with the homology-modeled protein structure. Bioorg Med Chem 16:284–292
Plant TD, Henquin JC (1990) Phentolamine and yohimbine inhibit ATP-sensitive K+ channels in mouse pancreatic β-cells. British J Pharmacol 101:115–120
Puls W, Keup U, Krause HP, Thomas G, Hoffiester F (1977) Glucosidase inhibition. Naturwisenschaften 64:536–537
Reuser AJ, Wisselaar HA (1994) An evaluation of the potential side-effects of α-glucosidase inhibitors used for the management of diabetes mellitus. Eur J Clin Invest 24:19–24
Samad AH, Willing TST, Alberti KGM, Taylor R (1988) Effects of BAYm 1099. New alpha-glucosidase inhibitor on acute metabolic responses and metabolic control in NIDDM over 1 month. Diabetes Care 11:337–344
Scheen AJ (2003) Is there a role for α-glucosidase inhibitors in the prevention of type 2 diabetes mellitus? Drugs 63:933–951
Schmidt D, Frommer W, Junge B, Muller L, Wingender W, Truscheit E, Schäfer D (1977) alpha-glucosidase inhibitors. New complex oligosaccharides of microbial origin. Naturwissenschaften 64:535–536
Schrödinger Release 2015-1: Maestro, version 10.1, Schrödinger LLC, (2015) New York, NY
Scott LJ, Spencer CM (2000) Miglitol. Drugs 59:521–549
Shim YJ, Doo HK, Ahn SY, Kim YS, Seong JK, Park IS, Kim BH (2003) Inhibitory effect of aqueous extract from the gall of Rhus chinensis on alpha-glucosidase activity and postprandial blood glucose. J Etnhopharmacology 85:283–287
Storr SJ, Royle L, Chapman CJ, Hamid UMA, Robertson JF, Murray A, Dwek RA, Rudd PM (2008) The O-linked glycosylation of secretory/shed MUC1 from an advanced breast cancer patient's serum. Glycobiology 18:456–462
Taha M, Ismail NH, Imran S, Ali M, Jamil W, Uddin N, Kashif SM (2016a) Identification of bisindolylmethane–hydrazone hybrids as novel inhibitors of β-glucuronidase, DFT, and in silico SAR intimations. RSC Adv 6:3276–3289
Taha M, Ismail NH, Imran S, Selvaraj M, Rahim F (2016b) Synthesis of novel inhibitors of β-glucuronidase based on the benzothiazole skeleton and their molecular docking studies. RSC Adv 6:3003–3012

Taha M, Ismail NH, Javaid K, Imran S, Wadood A, Ali M, Khan KM, Saad SM, Rahim F, Choudhary MI (2015a) Evaluation of 2-indolcarbohydrazones as potent α-glucosidase inhibitors, in silico studies and DFT based stereochemical predictions. Bioorg Chem 63:24–35

Taha M, Ismail NH, Lalani S, Fatmi MQ, Siddiqui S, Khan KM, Imran S, Choudhary MI (2015b) Synthesis of novel inhibitors of α-glucosidase based on the benzothiazole skeleton containing benzohydrazide moiety and their molecular docking studies. Eur J Med Chem 92:387–400

Taha M, Ismail NH, Imran S, Wadood A, Rahim F, Ali M, Rehman AU (2015c) Novel quinoline derivatives as potent in vitro α-glucosidase inhibitors: in silico studies and SAR predictions. Med Chem Comm 6:1826–1836

Taha M, Ismail NH, Imran S, Rahim Mohamad MH, Wadood A, Rahim F, Saad SM, Rehman A, Khan KM (2016) Synthesis, α-glucosidase inhibitory, cytotoxicity and docking studies of 2-Aryl-7-methylbenzimidazoles. Bioorg Chem 65:100–109

Tang PC, Lin ZG, Wang Y, Yang FL, Wang Q, Fu JH, Zhang L, Gong AS, Luo JJ, Dai J, She GH, Si DD, Feng J (2010) Design and synthesis of DPP-4 inhibitor for the treatment of type 2 diabetes. Chin Chem Lett 21:253–256

Taylor SI, Accili D, Imai Y (1994) Insulin resistance or insulin deficiency. Diabetes 43:735–740

Porte Jr. D (1991) Beta-cells in type II diabetes mellitus. Diabetes 40:166–180

Temple Jr. C, Rose JD, Comber RN, Rene GA (1987) Synthesis of potential anticancer agents: imidazo [4, 5-c] pyridines and imidazo [4, 5-b] pyridines. J Med Chem 30:1746–1751

Verdonk ML, Cole JC, Hartshorn MJ, Murray CW, Taylor RD (2003) Improved protein-ligand docking using GOLD. Proteins 52:609–623

Wang YF, Yang ZW, Wei XL (2010) Sugar compositions, α-glucosidase inhibitory and amylase obtained by different extraction methods. Int J Biol Macromol 47:534–539

Wehmeier UF, Piepersberg W (2004) Biotechnology and molecular biology of the α-glucosidase inhibitor acarbose. Appl Microbiol Biotech 63:613–625

Whiting DR, Guariguata L, Weil C, Shaw J, ((2011) IDF diabetes atlas: global estimates of the prevalence of diabetes for 2011 and 2030. Diabetes Res Clin Pract 94:311–321

Wu YH (2007) Synthesis of (S) 2-ethoxy-3-phenylpropanoic acid derivatives and their insulin sensitizing activity. Chin J Chem 25:265–267

Zawawi NKNA, Taha M, Ahmat N, Ismail NH, Wadood A, Rahim F (2017) Synthesis, molecular docking studies of hybrid benzimidazole as α-glucosidase inhibitor. Bioorg Chem doi:10.1016/j.bioorg.2016.12.009